西交利物浦大學
Xi'an Jiaotong-Liverpool University

EEE213 Power Electronics and Electromechanics

Report on Lab: Single-phase Half-wave and Full-wave Controlled Rectification Circuit

Name: Yukun.Zheng
ID Number: 2251625

Content:

1. Introduction

a) Overview and Relevance

This power electronics experiment aims to explore the working characteristics and control methods of single-phase controllable rectifier circuits. The lab is divided into two parts, which are Single-phase half-wave Controllable Rectifier Circuit and Single-phase Fully Controlled Bridge rectifier/Inverter Circuit, requiring students to finish them separately at week 8 and week 9. By wiring and testing these two types of typical rectifier circuits, students will have a thorough understanding of the application mode of thyristors in AC-DC conversion, and perform the phase control by modifying the firing angle on the output voltage. Rectification technology, as a fundamental content in power electronics, has extensive application value in multiple engineering fields such as motor control, renewable energy interfaces, and power management.

b) Objectives of the Experiment

There are several objectives of this experiment. Firstly, students have to master the methods of UJT triggering circuits and linear angle controlling circuits by modifying variable resistors Rp and oscilloscope. Secondly, they observe and measure the variation trend of the rectifier output voltage under different control angle α conditions. Thirdly, students analyze the difference of output waveforms between pure resistive load and inductive load.

2. Background knowledge

This chapter will review the theoretical basis related to this experiment and is divided into two parts: Firstly, it introduces the principle of rectifier circuits taught in the classroom, including the working mechanisms of single-phase half-wave and single-phase full-wave controllable rectifier circuits. Secondly, supplement the extracurricular knowledge required for the experiment, with a focus on explaining the physical process and functional characteristics of the UJT trigger circuit and the linear control angle trigger circuit. These knowledge together constitute the theoretical basis for the understanding and operation of this experiment.

※2.1 Lecture knowledge review: Basic principles of single-phase controlled rectifier

a) Single-phase half-wave controllable rectifier circuit

The single-phase half-wave controllable rectification refers to the regulation of the

output voltage by controlling the conduction time of the thyristor during the positive half-cycle of the AC voltage.

- R load

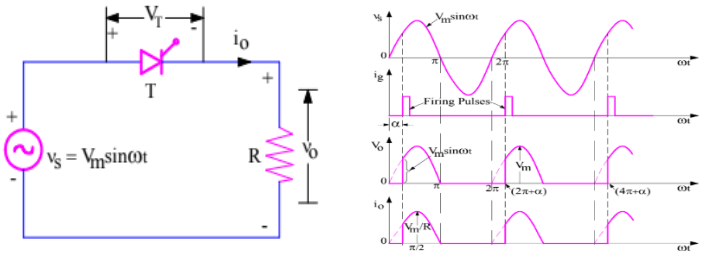

Figure 1: Single-phase half-wave controlled rectifier schematic (resistive load)

In a single-phase half-wave controllable rectifier circuit, the thyristor (SCR) is only triggered to conduct within the positive half-cycle of the AC input voltage. The conduction duration is adjusted by controlling its trigger angle α, thereby regulating the average value of the output voltage. Before being triggered, the thyristor is in the cut-off state and the voltage across the load is zero. When the control angle α is reached, the trigger pulse acts to conduct the thyristor, and the output voltage begins to follow the input voltage until the end of the half-cycle. Under the R load, the current is synchronized with the output voltage, presenting a single half-wave sinusoidal form and conducting periodically.

- RL load

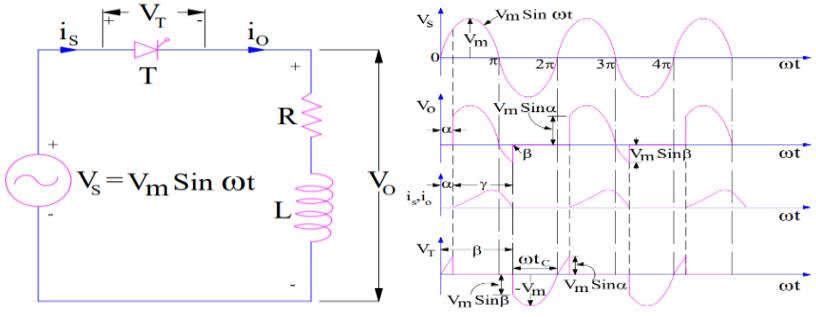

Figure 2: Single-phase half-wave controlled rectifier schematic (inductive load)

When inductive components are introduced into the load, the energy storage effect of the inductor will affect the cut-off time of the current. Although the thyristor is still triggered in the positive half-cycle, due to the release of inductor energy storage, the current will continue to flow after the input voltage crosses zero, forming a continuation current phenomenon. At this point, the output voltage will also continue a attenuation waveform after crossing the zero point until the natural turn-off angle β. Under the same α, the average output voltage under RL load is usually higher than

that under pure resistive load, and the waveform is also smoother.

b) Single-phase fully controlled bridge rectifier circuit

Compared with half-wave rectification, the fully controlled bridge rectifier circuit uses four thyristors to form a bridge connection in structure, which can respectively control the rectification process of the positive and negative half-cycles.

- R load

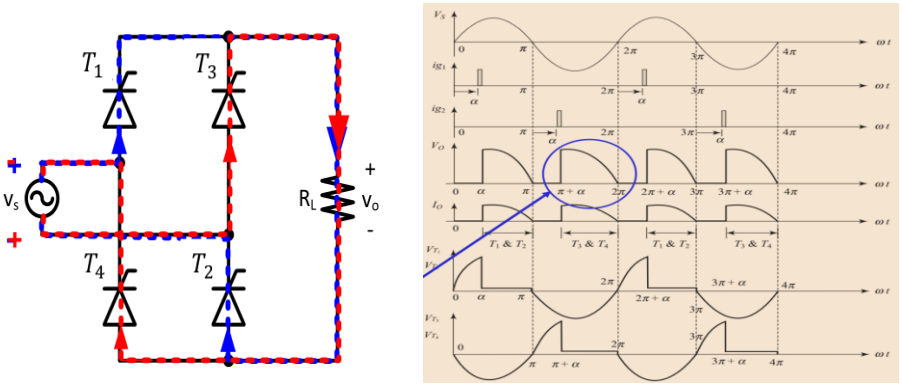

Figure 3: Single-phase full bridge rectifier schematic (R load)

The full-bridge rectifier circuit is composed of four thyristors. By controlling the conduction of two thyristors respectively in the positive and negative half-cycles, full-wave rectification is achieved. Within each half-cycle, the control angle α determines the starting point of conduction. Conduction is carried out until the end of the half-cycle, achieving alternating conduction of positive and negative half-waves, and the output waveform is a full-wave pulsating DC with periodic continuity. Under pure resistive load, the load voltage waveform is synchronized with the input voltage waveform. Each conduction starts from α and ends at π or 2π. Since both half weeks can be effectively utilized, the average output voltage and power are higher.

- RL load

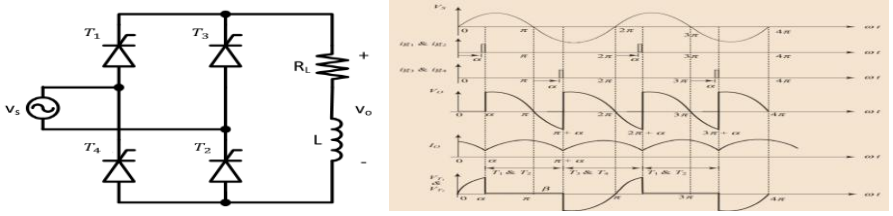

Figure 4: Single-phase full bridge rectifier schematic (RL load)

Before analyzing, it is noted that the default extinction angle β satisfies $\beta < \pi + \alpha$.
Under inductive loads, the current also lags due to inductive effects. Even if the voltage has crossed zero, the current may still persist, causing the output voltage to be continuously delayed until the natural turn-off angle β. Two sets of thyristors alternately conduct and automatically cut off when the load current is lower than the holding current, forming a more stable current transition process. Compared with half-wave rectification, full-wave bridge rectification has a more continuous output waveform and a higher average voltage under RL load, making it more suitable for applications with high requirements for output stability.

※2.2 Supplementary pre-lab knowledge: Basic principles of two typical firing circuits

a) The principle of UJT firing circuit

- UJT basics

UJT (Uni-Junction Transistor) is a three-terminal semiconductor device with negative resistance characteristics and is widely used in trigger circuits. Its working principle and characteristics can be illustrated by the following three sub-diagrams:

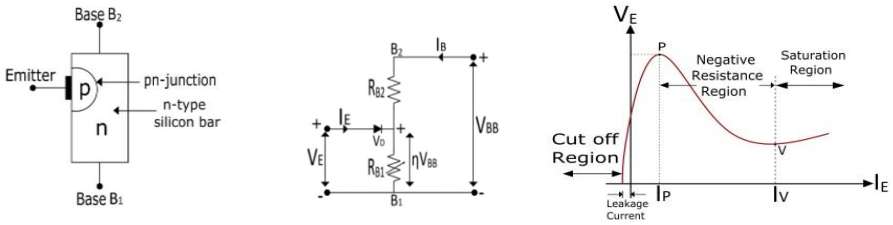

Figure 5. Unijunction Transistor (UJT) characteristics: (a) Physical structure of the UJT. (b) Equivalent circuit model. (c) Voltage-current (V–E) characteristic curve showing cutoff, negative resistance, and saturation regions.

1. Physical structure (Figure 5a)

The structure of a UJT is to incorporate a P-type region in the center of an N-type silicon strip, with the three terminals corresponding to the base B2, emitter E and base B1 respectively. Two PN junctions are formed between the p region and the silicon strip. Among them, the E-B1 junction is used for triggering, and the B2 terminal maintains a high potential bias.

2. Equivalent Circuit and Bias (Figure 5b)

The applied bias voltage VBB is crossed between B2 and B1 through the resistor network (RB2, RB1), and the emitter E is connected to the voltage divider junction. When the voltage VE of E-B1 reaches the conduction voltage VD of the PN junction, the emitter current IE begins to flow in and is affected by the voltage division of the resistors across the terminals.

3. V-E Characteristic Curve (Figure 5c)
The VE-IE curve is divided into three regions:
✧ Cut-off Region:
IE is very small, only the leakage current dominates.
✧ Negative Resistance Region:
When IE increases to the voltage VP corresponding to the peak IP, VE decreases instead after the UJT conducts, forming a negative resistance characteristic.
✧ Saturation Region:
After IE increases to IV, the device enters saturation, and VE continues to increase slightly along with IE.
These three parts briefly explain how a UJT, through its own negative resistance region characteristics, generates sharp pulses when the trigger capacitor discharges to drive the thyristor gate.

- UJT firing circuit analysis

In this experiment, UJT forms an RC charge-discharge network with external resistors and capacitors. After startup, capacitor C begins to charge slowly. When the charging voltage reaches Vp, UJT conducts in the negative resistance region, and C discharges rapidly, triggering the transformer to output a high-frequency pulse signal. Subsequently, the UJT turned off due to the voltage dropping to the valley of the Uv and entered the next round of charging process.
By adjusting the potentiometer RP, the RC time constant can be changed, thereby precisely adjusting the conduction moment of the UJT, that is, controlling the trigger angle α of the thyristor. This structure features self-excited oscillation and periodic stability, and it is an important fundamental means to achieve the control angle adjustment of single-phase controllable rectifiers.

b) The principle of linear control angular trigger circuit
The linear control angle trigger circuit achieves precise conduction control of the thyristor by comparing the sawtooth wave with the reference level. The basic principle is as follows: The AC synchronous signal provides a zero-point reference, and the constant current source charges the capacitor C to form a linearly rising sawtooth wave. When the sawtooth wave voltage rises to the set reference level (determined by RP2 and RP3), the comparator processes and outputs a pulse signal, causing the thyristor to conduct.
This circuit has stronger adjustability and linear accuracy compared with the UJT

scheme, and is suitable for bidirectional control with higher requirements for symmetry and accuracy, such as the alternating triggering of dual thyristors in full-bridge rectifier circuits.

3. Experiment procedure and results

This chapter presents the specific implementation process and obtained results of this power electronics experiment, divided into two major parts: Experiment One—single-phase half-wave controllable rectifier circuit—and Experiment Two—single-phase fully controlled bridge rectifier circuit. Each experiment involves two key procedures: debugging the trigger circuit and performing measurements with a multimeter alongside oscilloscope waveform calibration. Accordingly, the operation steps required by the experimental manual are listed, followed by the experimental data and waveform screenshots. The theoretical and measured values are then calculated and compared. Finally, a brief explanation of the key phenomena is given.

Note that this chapter is limited to presenting results and brief analysis only, and for detailed analysis, see Chapter 4. To keep the report concise, this chapter includes only the feedback results from trigger-circuit testing, the multimeter measurements and oscilloscope waveform results for Experiment 1.

※3.1 Experiment 1: Single-phase Half-wave Controlled Rectification Circuit

- Step 1: UJT firing circuit testing

Before formal measurement, it is suggested that students need to check and verify the UJT firing circuit functioning normally. Therefore, I recorded the output waveforms of all terminals and displayed the waveform in the oscilloscope shown as below when I controlled the firing angle to 60 degrees by changing Rp.

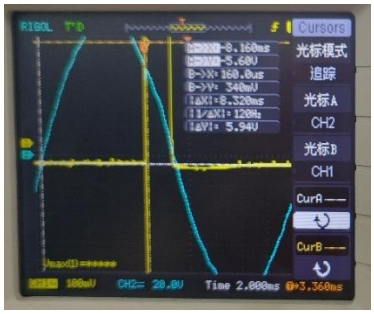

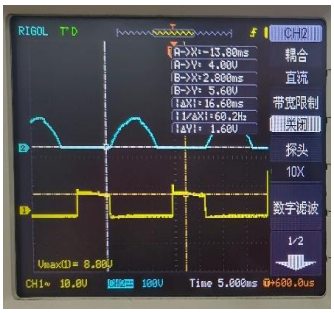

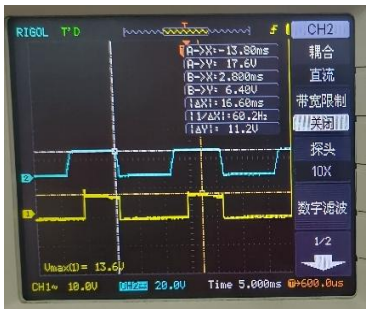

Figure 6: Oscilloscope waveforms of key voltages in the circuit:
(a) U voltage. (b) VT1 voltage. (c) VT2 voltage. (d) VT3 voltage. (e) VT4 voltage. (f) VT5 voltage. (g) GK voltage.

Fortunately, the waveforms corresponded to our expectations.

➢ Step 2: Wiring and R load measurement

After comparing and verifying the obtained waveforms on the oscilloscope, I started building the circuit on the lab instrument.

- Wiring method

In the experiment under R load, first, according to the experimental manual, the SCR, two parallel 900 Ω resistors and the UJT trigger circuit were successively connected to the MPE-01, MPE-12 and MPE-25 panels. And mark the corresponding relationships between TP1, TP5, G/K terminals and the oscilloscope channels on the panel. Subsequently, channel 1 of the oscilloscope is connected to TP1 for observing the synchronization reference signal, and channel 2 is connected to TP5 or the output terminal Vo for capturing the trigger pulse or rectification waveform. The multimeter is respectively switched to the AC RMS mode to measure U_2 and the DC voltage mode to measure Ud.

- Firing angle control method

To determine the actual firing angle from the captured waveforms, the following procedure was applied: given a line frequency of $f = 50\,Hz$, the angular frequency is $\omega = 2\pi f = 100\pi\,rad/s$, and the instantaneous phase angle satisfies $\theta = \omega t$. Adjusting RP1 therefore varies the delay time t before the SCR fires. On the oscilloscope, two cursors were placed—one at the reference zero-crossing of the AC input and the other at the leading edge of the trigger pulse—so that the time difference Δt between them could be read directly. This time delay corresponds to a phase shift of $\Delta\theta = \omega\,\Delta t\,rad$, which is then converted to degrees via $\Delta\theta^\circ = \Delta\theta \times (180^\circ/\pi)$.

Applying this conversion for each setpoint yields the table below, listing the nominal

firing angles alongside their measured time delays.

α(°)	30	60	90	120	150
Δt(s)	1.67m	3.33m	5.00m	6.67m	8.33m

Table 1: Firing angles (α) and corresponding time delays (Δt)

- Voltage Measurement & Comparison

The measured results after operation and comparison between ideal and practical cases are shown as below where $Ud = \frac{Vm(1+cos\alpha)}{2\pi}$, and $Vm = 220 * \sqrt{2} = 311\ v$

α(°)	30	60	90	120	150
U2 (Practical) (V)	230	230	230	230	230
Ud (Practical value) (V)	108.8	92.2	65.6	31.39	14.19
Ud (Practical)/U2	0.473	0.401	0.285	0.136	0.062
U2 (Theoretical) (V)	220	220	220	220	220
Ud (Theoretical) (V)	92.4	74.3	49.5	24.8	6.6
Ud (Theoretical)/U2	0.420	0.338	0.225	0.113	0.030

Table 2: Practical and theoretical voltage values at different firing angles (R load)

In this section, I will provide some screenshots of the multimeter and oscilloscope to support my data.

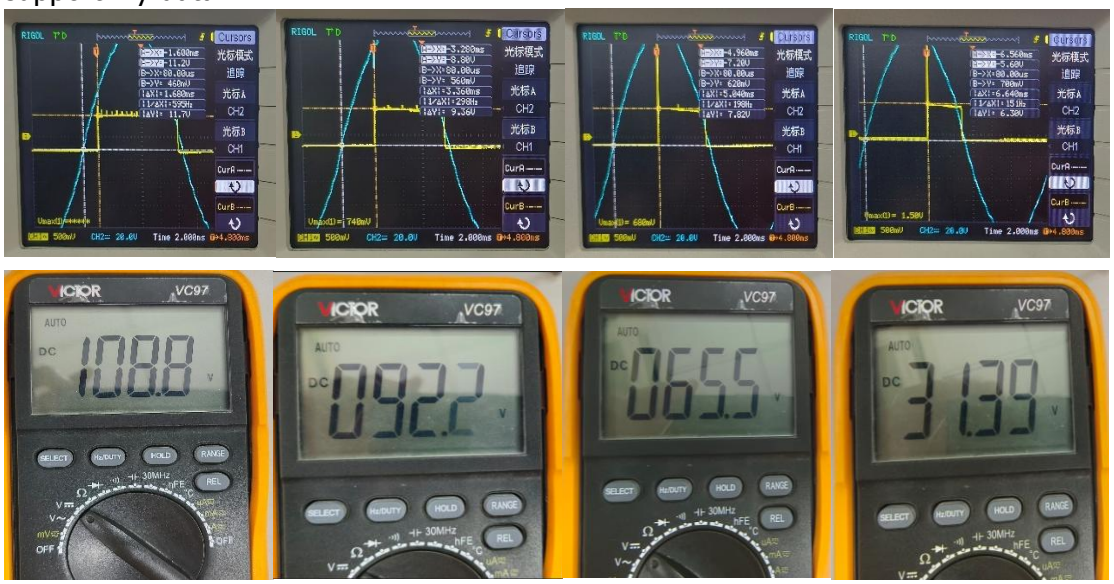

Figure 7: Digital multimeter measurements & oscilloscope waveforms

Note that here, only the data in the table is presented. For a detailed analysis, see chapter 4.

➢ Step 3: Wiring and RL load measurement

- Wiring method

Since wiring procedures are provided on the lab script and I have demonstrated my wiring method in step 2, to reduce redundancy, I omitted the analysis here.

- Firing angle control method

Since Experiment 1 still requires UJT firing circuit, thus the firing angle control method remains the same as the R load analysis. For simplicity, I omit the same analysis here to keep brevity.

- Voltage Measurement & Comparison

The measured results after operation and comparison between ideal and practical cases are shown as below where $Ud = \frac{Vm(cos\alpha - cos\beta)}{2\pi}$, $Vm = 220 * \sqrt{2} = 311\ v$, $\sin(\alpha - \varphi) * e^{-\frac{\beta-\alpha}{\tan(\varphi)}} = \sin(\beta - \alpha)$, and $\varphi = arctan(\omega L/R)$.

α(°)	30	60	90	120	150
U2 (Practical) (V)	230	230	230	230	230
Ud (Practical value) (V)	108.4	97.7	75.7	35.27	13.95
β(°)	193.7299	193.7271	193.6962	193.4403	191.7180
Ud (Theoretical) (V)	90.99	72.86	48.11	23.40	5.22

Table 3: Practical and theoretical voltage values at different firing angles (RL load)

Note that here, only the data in the table is presented. For a detailed analysis, see chapter 4.

※3.2 Experiment 2: Single-phase Full-controlled Rectification Circuit

➢ Step 1: Linear firing angle control circuit testing

Since Experiment 1 shares almost the same firing angle control principle with experiment two (by modifying Rp and cursors on the oscilloscope), thus for simplicity, I omit the same analysis here to keep brevity.

➢ Step 2: Wiring and R load measurement

After comparing and verifying the obtained waveforms on the oscilloscope, I started building the circuit on the lab instrument.

- Wiring method

Since wiring procedures are provided on the lab script and I have demonstrated my wiring method in previous analysis, to reduce redundancy, I omitted the analysis here.

- Firing angle control method

In experiment 2, I modified RP3 first, then Rp1 and RP2 last to obtain control the firing angle. According to my observation, I found that the slope of the sawtooth wave is sensitive to the change of Rp1, and Rp2 is responsible for generating a reference voltage for the sawtooth wave to compare in order to generate the impulse signal, where this concept is covered in lecture 10 P20.

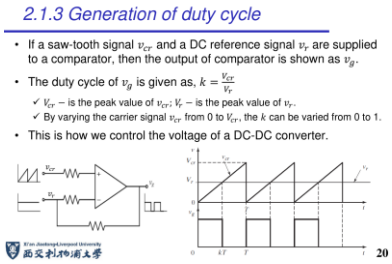

Figure 8: Duty cycle generation mechanism

Rp3 can be used to control the value of the firing angle.

Note that table 1 still holds validity for this experiment.

- Voltage Measurement & Comparison

The measured results after operation and comparison between ideal and practical cases are shown as below where $Ud = \frac{Vm(1+cos\alpha)}{\pi}$, and $Vm = 220 * \sqrt{2} = 311\ v$

α(°)	30	60	90	120
U2 (Practical) (V)	245	245	245	245
Ud (Practical value) (V)	211	185.4	122	74
Ud (Practical)/U2	0.861	0.757	0.498	0.302
U2 (Theoretical) (V)	220	220	220	220
Ud (Theoretical) (V)	184.6	148.5	99.0	49.5
Ud (Theoretical)/U2	0.839	0.675	0.450	0.225

Table 4: Practical and theoretical voltage values at different firing angles (R load)

Note that here, only the data in the table is presented. For a detailed analysis, see chapter 4.

➢ Step 3: Wiring and RL load measurement

- Wiring method

Since wiring procedures are provided on the lab script and I have demonstrated my wiring method in step 2, to reduce redundancy, I omitted the analysis here.

- Firing angle control method

Since the method is the same as shown in step 2. For simplicity, I omit the same

analysis here to keep brevity.

- Voltage Measurement & Comparison

The measured results after operation and comparison between ideal and practical cases are shown as below where

$$Ud = \frac{1}{\pi} * [\int_{\alpha}^{\beta} Vm * \sin(\omega t)\, d\omega t] = \frac{Vm*[\cos(\alpha)-\cos(\beta)]}{\pi}$$

$$Vm = 220 * \sqrt{2} = 311\, v,\ \sin(\alpha - \varphi) * e^{-\frac{\beta-\alpha}{\tan(\varphi)}} = \sin(\beta - \alpha),$$

and $\varphi = arctan(\omega L/R)$.

α(°)	30	60	90	120
U2 (Practical) (V)	243	243	243	243
Ud (Practical value) (V)	205	171	121	69
β(°)	193.7299	193.7271	193.6962	193.4403
Ud (Theoretical) (V)	181.9	145.66	96.18	46.19

Table 5: Practical and theoretical voltage values at different firing angles (RL load)

Note that here, only the data in the table is presented. For a detailed analysis, see chapter 4.

4. Results analysis and discussion

In the previous chapter, we have elaborated on the circuit wiring of Experiment 1 and Experiment 2 under R load and RL load conditions, the measurement methods of oscilloscopes and multimeters, as well as the experimental results and waveform screenshots under each working condition.

This chapter will conduct a systematic comparison and analysis of the output characteristics of the single-phase half-wave controllable rectification in Experiment One and the single-phase fully controlled bridge rectification in Experiment Two under the conditions of R load and RL load. For the sake of clear logic, the discussion is divided into two major parts:

1. Comparison of half-wave vs. full-wave rectification characteristics under R load
2. Comparison of half-wave vs. full-wave rectification characteristics under RL load

By comparing the trend of Ud/U_2 varying with the trigger angle α under different rectification methods and load types, the conduction and off characteristics of the output waveforms, as well as the deviation between the theoretical and measured results, the aim is to reveal the influence of inductance on the rectification process and the error sources of the thyristor trigger circuit.

- ➢ R load comparisons & explanations
- ● Data Analysis
- ✧ General tendency evaluation

Because the two experiments were carried out in different weeks using different instruments, the raw source voltages I recorded are not directly comparable. To overcome this, we instead evaluate the rectification performance by examining the ratio $Ud/U2$. The table below presents the values of their ratios, collected from the measurements reported in the previous chapter.

α (°)	Half-wave (V) Ud/U₂(practical)	Half-wave (V) Ud/U₂(ideal)	Full-wave (V) Ud/U₂(practical)	Full-wave (V) Ud/U₂(ideal)
30	0.473	0.420	0.861	0.839
60	0.401	0.338	0.757	0.675
90	0.285	0.225	0.498	0.450
120	0.136	0.113	0.302	0.225
150	0.062	0.030	—	—

Table 6: General comparison of $Ud/U2$ ratios under different firing angles for half-wave and full-wave rectification (R load)

Under the condition of the same trigger angle α, the output voltage ratio Ud/U_2 of full-wave rectification is almost twice that of half-wave rectification. This can be fully reflected in the measured data: for example, when $\alpha = 30°$, the measured Ud/U_2 of half-wave is approximately 0.473, while that of full-wave is approximately 0.861, which fully demonstrates that full-wave rectification utilizes the energy of both the positive and negative half-cycles. And formula of full wave $Ud/U2 = (2/\pi) * [1 + \cos(\alpha)]$ is equal to 2 times half wave $Ud/U2 = (1/\pi) * [1 + \cos(\alpha)]$, verified the advantage.

- ● Error tracking
- ✧ System Errors

1. Measurement error

- ✓ Cause and Description:

The scale accuracy of oscilloscopes and multimeters is limited, and the readings of RMS voltmeters are usually slightly higher than the nominal value of 220 V, resulting in a systematic increase in all Ud/U_2 ratios.

- ✓ Impacts:

The measured U_2 and Ud constantly deviate from the true values, resulting in a fixed difference between the measured ratio and the theoretical ratio.

2. Non-ideal characteristics of the device

- Cause and Description:

In the ideal model, we assume that when the thyristor is on, there is no voltage drop and the conduction angle α is exactly the same as the trigger angle. At the moment of turn-off, the voltage immediately jumps to the opposite of the peak value of the source voltage. However, when the SCR is actually on, there is a typical voltage drop about 1-2 V, which directly offsets the voltage that can be obtained on the load during the conduction period. Furthermore, when the AC voltage crosses zero and enters the next half of the cycle, the SCR does not immediately turn off. Instead, there is a brief lag in the continuation current, and it will only cut off when the load current drops below the holding current.

✓ Impacts:

Let us demonstrate this concept with the two circuits respectively.

A. Half-wave controllable Rectifier circuits

In the full-bridge rectifier circuit, two SCRS are conducted in series in each half cycle, so the voltage drop becomes approximately $2VT$. Ideal full-wave average output is

$$Ud = \frac{Vm(1 + cos\alpha)}{2\pi}$$

Assuming no voltage drop, but after actual conduction, the load can only obtain a voltage of $Vs - VT$, which reduces the measured Ud by a fixed amount VT/π, and thereby systematically improves the ratio deviation of $Ud/U2$. In addition, when the half-wave rectifier crosses zero during the positive half-week, theoretically, the SCR should be turned off immediately. However, in reality, the current still needs to flow through the parasitic component of the inductor or the residual energy of the load to drop below the holding current, resulting in an extremely short trailing current lag. This causes the half-waveguide's passable region to slightly exceed π, further increasing the actual average voltage.

B. Full-wave controllable Rectifier circuits

In the full-wave rectifier circuit, only one SCR conducts in each conduction cycle. During the conduction period, the voltage drop VT≈2v is equivalent to the voltage loss on the load. Ideally, the average output voltage formula

$$Ud = \frac{Vm(1 + cos\alpha)}{\pi}$$

Assuming no voltage drop, but after actual conduction, the load obtains a voltage of $Vs - 2VT$, making Ud systematically less than the ideal value by $2 * VT/\pi$. Due to the conduction of the two SCRs, the error is more obvious than the single-thyristor

voltage drop effect of the half-wave, but compared with the higher output voltage of the full-wave, the proportion of this fixed loss is slightly smaller instead. In addition, the shutdown of any half of the weekend in the full bridge also needs to wait for the load current to drop below the holding current before it can be cut off. Especially in RL loads, the double trailing current lag slightly extends the length of each half wave of the output waveform, further deviating from the ideal cut-off point, thereby causing a systematic upward shift in the average voltage.

3. Parasitic effect and impedance

- Cause and Description:

Under our ideal assumption, the tiny parasitic components among the wires, capacitors and inductors are ignored. However, in actual hardware wiring, the wires themselves have distributed inductance, the test leads and oscilloscope probes have capacitance, as well as the contact resistance at each contact point. All these constitute a complex high-frequency parasitic network.

✓ Impacts:

A. Parasitic effect

In actual circuits, wires, capacitors, inductors and test instruments inevitably introduce parasitic capacitors and parasitic inductors, especially at the edges where the trigger pulses and output voltages change rapidly, the impact is significant. In half-wave rectification, parasitic capacitance will passivate the pulse leading edge and weaken the triggering accuracy. In full-wave rectification, the positive and negative half-cycles alternate in conduction, and the parasitic capacitance effect superimposes, which easily causes tailing and deformation of the conduction waveform and reduces the accuracy of the output voltage. In addition, parasitic inductance can cause an additional voltage drop when the current suddenly changes, affecting the actual load voltage during the conduction of the SCR.

B. Impedance influence

The contact resistance and wiring complexity in the actual wiring process lead to the existence of non-ideal distributed impedance in the line. The half-wave rectification path is simple, and the additional resistors are mainly concentrated in a single SCR branch. In full-bridge rectification, the current needs to pass through two SCRS and multiple nodes. Each conduction path is longer, and the resistance superposition is significant, resulting in a relatively obvious voltage loss. This structural difference leads to the fact that full-wave rectification is more prone to systematic low voltage in actual measurements.

✧ Random Errors

1. Unstable trigger pulse and time base of the oscilloscope

- Cause and description

The oscilloscope's synchronous trigger technology and internal sampling have slight jitter. The larger the trigger angle and the narrower the pulse, the time base cursor resolution limit during measurement causes slight fluctuations in the reading between different acquisitions.

✓ Impacts:

A. Half-wave controllable Rectifier circuits

In a half-wave rectifier circuit, since there is only one trigger pulse per cycle and the pulse width is already very narrow, the synchronous trigger jitter of the oscilloscope and the resolution limit of the time base cursor will cause more obvious random fluctuations when measuring Δt : The trigger delay time obtained from one measurement may differ by several microseconds from the next one, resulting in a random deviation of ± several degrees or ± several percentages in the trigger angle and Ud/U_2 calculated by $\alpha = \omega * t$.

B. Full-wave controllable Rectifier circuits

In contrast, full-wave rectification has two trigger pulses per cycle. Although individual pulses are also affected by time base jitter, the average effect of the two pulses compensates for each other to a certain extent - the slight shake of the first and second trigger angles sometimes offsets each other, making the overall measurement fluctuation of Ud/U_2 slightly smaller than that of the half-wave case. Therefore, in half-wave experiments, it is even more necessary to suppress random errors by capturing individual pulses multiple times and averaging them. In full-wave experiments, it is also recommended to measure the positive and negative half-cycles multiple times respectively and then average them to further improve the measurement stability.

C. Abnormal statistics

To further evaluate the effect due to this random error, here I also establish a new table with relative error formulated as

$$Relative\ Error = \frac{Ud_{pratical} - Ud_{ideal}}{Ud_{ideal}}$$

α (°)	Half-wave (%) Relative error	Full-wave (%) relative error
30	12.6	2.6
60	18.6	12.7
90	26.6	10.7
120	20.4	34.2
150	106.7	—

Table 7: Relative error of R load under half-wave and full-wave conditions

From this table, it is obvious that under the two working conditions of half-wave $\alpha = 150^\circ$ and full-wave $\alpha = 120^\circ$, the measurement error is the most prominent, far exceeding other points. This kind of error that occurs at an extremely small output voltage with a very narrow pulse width mainly results from the measurement instability caused by the cursor resolution of the oscilloscope and the reading jitter of the multimeter, and it belongs to random error. Because they are not constant deviations but occasional fluctuations that occur when the signal amplitude is extremely small, there is a large random deviation between a single measurement value and the true value. Other more stable and consistent pressure drop deviations still fall within the category of systematic errors.

- Circuit characteristics summary

Furthermore, we can recall the principles of single-phase controlled rectifier circuits that the half-wave rectification conducts only in the positive half-cycle, the output waveform interval is obvious, and the DC component Vo is discontinuous. Full-wave rectification, on the other hand, remains conducting for both half-cycles, resulting in a denser and more continuous waveform. Therefore, under the same load conditions, the average power output is almost twice that of a half-wave, and the DC output is also smoother and more stable. Such characteristics make full-wave rectification more advantageous in situations that require high efficiency, while half-wave rectification is suitable for applications with lower requirements for output quality due to its simple structure.

➢ RL load comparison & explanations

- Beta Calculating method

✧ Ideal model

From the ideal model presented in the lecture slides of the single-phase half-wave controlled rectifier, we have the relationship as follows.

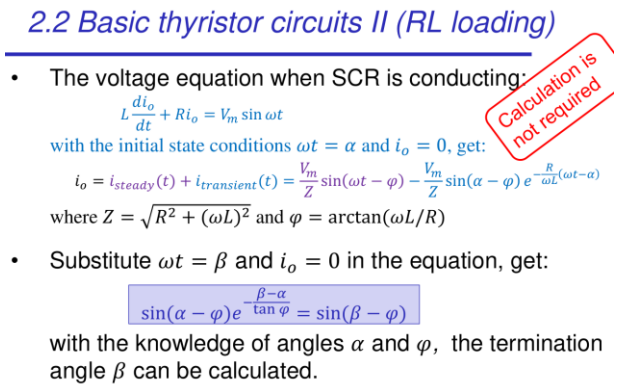

Figure 9: Beta calculation for single-phase half-wave controlled rectifier

Since we neglected the voltage drop of SCR, thus we can directly use this formula to calculate. However, due to the non-linear mathematic relations, we have to solve the beta in MATLAB using function calling method. Since this equation cannot be analytically solved, the fzero numerical root function in MATLAB is adopted for solution. My program contains two scripts:

※Main function runCalcBeta.m: Prompts the user to input the conduction angle α (unit: degrees), and calls the calculation function to output the corresponding β value.

※Subfunction calcBeta.m: Converts the angle unit to radians and sets the initial guess value.

Running the codes, the result will be visualized as follows *(See codes in appendix)*.

```
>> runCalcBeta
Enter firing angle α (in degrees): 30
When α = 30.00°, the calculated β = 193.7299°
>> runCalcBeta
Enter firing angle α (in degrees): 60
When α = 60.00°, the calculated β = 193.7271°
>> runCalcBeta
Enter firing angle α (in degrees): 90
When α = 90.00°, the calculated β = 193.6962°
>> runCalcBeta
Enter firing angle α (in degrees): 120
When α = 120.00°, the calculated β = 193.4403°
>> runCalcBeta
Enter firing angle α (in degrees): 150
When α = 150.00°, the calculated β = 191.7180°
>>
```

Figure 10: MATLAB calculations of beta

✧ Practical model

In the ideal model, we assume that the voltage drop is zero when the thyristor is conducting, and derive the differential equation. However, in practice, there will be a voltage drop of 1 to 2V when the SCR is conducting. If it is a full-bridge rectification structure, there will be two SCRS (2 to 4V) on the conducting path every half cycle, and the voltage drop will be even higher. This voltage drop will cause the actual voltage

obtained by the load at the initial stage of conduction to be lower than the theoretical value, making the current establishment slower and thus delaying the actual position of the natural turn-off angle β. Therefore, if the ideal model formula is relied upon to calculate β without correcting the conduction voltage drop, a systematic deviation will occur, causing a fixed deviation between the theoretical β value and the observed value in the real waveform.

- Data Analysis

✧ General tendency evaluation

Follow the same logic, I create a new table here to present some statistics collected from previous chapter.

α (°)	Half-wave (V) Ud/U_2(practical)	Half-wave (V) Ud/U_2(ideal)	Full-wave (V) Ud/U_2(practical)	Full-wave (V) Ud/U_2(ideal)
30	0.471	0.414	0.844	0.827
60	0.425	0.331	0.703	0.662
90	0.329	0.219	0.498	0.437
120	0.153	0.106	0.284	0.213
150	0.060	0.024	—	—

Table 8: General comparison of $Ud/U2$ ratios under different firing angles for half-wave and full-wave rectification (RL load)

Under the RL load condition, whether it is half-wave rectification or full-wave rectification, Ud/U2 shows a monotonically decreasing trend with the increase of the trigger angle α, but the output efficiency of full-wave rectification is always significantly higher than that of half-wave rectification. For example, when α=30°, the measured full-wave Ud/U2 is approximately 0.844, while the half-wave is only 0.471. When α=120°, the half-wave value drops to approximately 0.153, while the full-wave remains at approximately 0.284. It can be seen that full-wave rectification can fully utilize the energy of the current tail wave in the positive and negative half-cycles, thereby ensuring that its average output voltage is always higher than that of half-wave rectification. Furthermore, by comparing with the theoretical values, it can be known that the measured data are basically consistent with the ideal values, verifying the rationality of the data and indicating that the experimental measurement has a good consistency with the theoretical derivation.

- Error tracking

✧ System Errors

1. Inaccurate modelling of the RL circuit

Cause and Description:

As mentioned in Abnormal data analysis, the ideal RL circuit model contradicts our discoveries in the lab. Therefore, the actual model should be built as the following figure (*take half-wave as an example*).

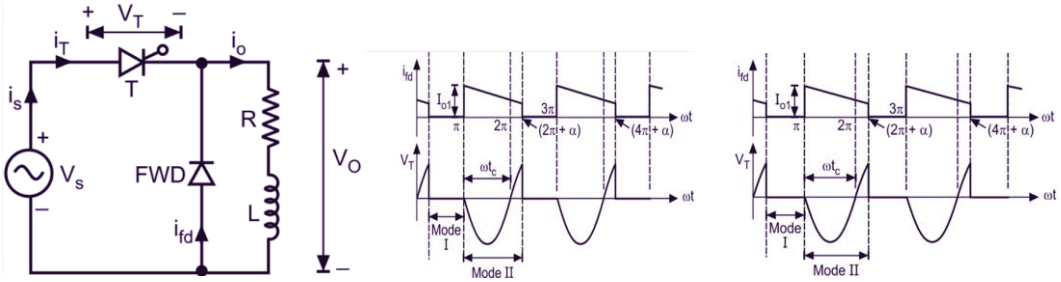

Figure 11: Single-phase half-wave controlled rectifier with RL load and freewheeling diode:
(a) Circuit diagram
(b) Waveforms of load current and voltage during Mode I and II
(c) Extended waveform analysis over multiple cycles

After adding a freewheeling diode to the half-wave controllable rectifier circuit, its operation can be divided into two stages.

※Mode I: Conduction Mode

When the trigger angle α arrives and a trigger pulse is applied to the gate of the thyristor (SCR), the SCR begins to conduct and remains in the conducting state until $\omega t = \pi$. At this point, the source voltage Vs is directly applied to the series-connected R-L load, and the load current io is provided by SCR. At this stage, the freewheeling diode is in the cut-off state, and the current path only passes through the SCR and the load. The output voltage is equivalent to the forward waveform of the half-wave rectification.

※Mode II: Continuation Mode

When $\omega t = \pi$, the source voltage enters the negative half-cycle, Vs reverses, resulting in a reverse voltage across SCR. At this point, since the energy stored in the load inductor L has not been completely released, io is still greater than the holding current of SCR, and SCR is still conducting. The reverse source voltage simultaneously causes the Freewheeling Diode to conduct forward, and the load current automatically transfers from the SCR to the freewheeling diode circuit to continue flowing. In this way, the energy in the inductor is fed back to the load through the freewheeling diode

instead of returning to the power supply, ensuring the continuity of the current. This stage lasts until the next trigger pulse arrives, and the load current gradually decays to zero.

✓ Impacts:

The above analysis is targeted for half-wave rectifier, however, the concept can still be applied to full-wave rectifier circuit as well.

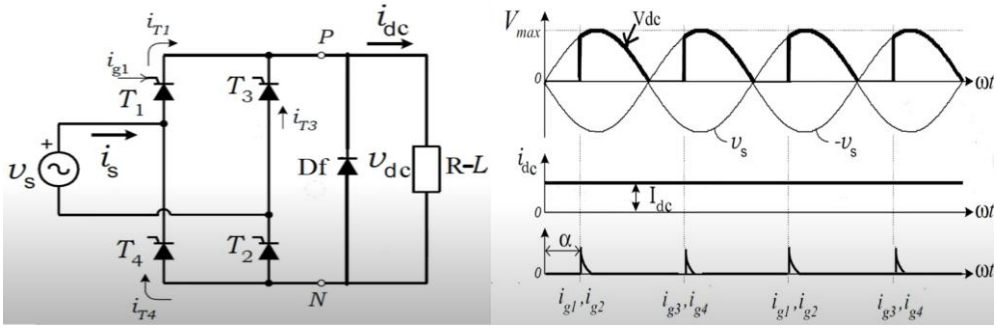

Figure 12: Single-phase full-wave controlled rectifier with RL load and freewheeling diode:
(a) Circuit diagram
(b) Voltage and current waveforms showing conduction intervals of switching devices

A. Half-wave controlled rectifier

For the error situation of half-wave rectification, the circuit and current waveform diagrams in Figure 1 can be referred to. The traditional ideal model assumes that the current is zero immediately after the thyristor is turned off, ignoring the current ripple (Mode II) caused by the energy released by the inductor in the RL load. In fact, after the thyristor is turned off, the freewheeling diode (FWD) will conduct, and the load current will enter the free freewheeling stage. During this stage, although the current decreases, it still persists for a period of time, resulting in the output voltage not ideally dropping to zero but remaining at a certain level. This phenomenon leads to the measured Ud/U2 being significantly higher than the theoretical value, especially at smaller trigger angles (such as 30°, 60°), because the decaying current after conduction (*or we call trailing current of the SCR due to the existence of freewheeling diode*) is longer and contributes more average voltage additionally. This is also one of the reasons why the actual value and the theoretical value deviates gradually as observed before.

B. Full-wave controlled rectifier

In full-wave rectification, the two SCRS conduct alternately. The current continuity

caused by the inductance ensures that the load current persists (free freewheeling) even after one pair of thyristors has completed conduction but before the other pair. This process is provided with a path by the freewheeling diode Df. This part of the continuation current contributes an additional average voltage value and is a source that has not been fully considered in theoretical calculations. Especially when the trigger angle is relatively large (such as 90° - 120°), the "charging" ability of the tail wave to the rectifier weakens, the error ratio increases, and the measured value is still slightly higher than the ideal value. The existence of this error source in full-wave rectification can be understood by analogy with the form of the slow decrease of current in Mode 2 of Figure 11.

The above two points fully demonstrate that if the ideal model does not consider the freewheeling diode and the freewheeling process of Mode II, it cannot accurately predict the actual rectification characteristics under RL load.

5. Conclusion

This experiment comprehensively investigated the working principles, circuit behavior, and performance characteristics of single-phase half-wave and full-wave controlled rectifiers under both resistive (R) and inductive (RL) loads. By constructing the circuits, adjusting the firing angles, and analyzing the voltage and current waveforms, we gained practical insights into how thyristor-based phase control affects the output characteristics of rectifiers.

Experimental results demonstrated a consistent trend: full-wave rectification provides a higher and more stable average output voltage compared to half-wave rectification, particularly under inductive load conditions. The influence of freewheeling currents, SCR voltage drops, and parasitic effects were critically discussed and quantified through theoretical models and simulation calculations. Notably, the turn-off angle β showed limited sensitivity to α in measured data due to system simplifications and measurement limitations, which were also interpreted as systematic and random errors.

Overall, this lab not only deepened our understanding of AC-DC conversion principles, but also trained us in waveform analysis, measurement interpretation, and practical circuit troubleshooting. These skills are essential for further exploration of power electronics applications in motor drives, renewable energy systems, and power control architectures.

6. Appendix

✧ calcBeta.m

```
function runCalcBeta()
% runCalcBeta  Demonstrates how to call calcBeta

  % Known ϕ (in degrees)
  phi = 13.73;

  % Read α (in degrees) from user input
  alpha = input('Enter firing angle α (in degrees): ');

  % Calculate β
  beta = calcBeta(alpha, phi);

  % Display result
  fprintf('When α = %.2f°, the calculated β = %.4f°\n', alpha, beta);
end
```

✧ runCalcBeta.m

```
function beta = calcBeta(alpha, phi)
% calcBeta  Calculates the turn-off angle β of SCR under RL load
%   beta = calcBeta(alpha, phi)
%   Inputs:
%     alpha - Firing angle α (in degrees)
%     phi   - Phase angle ϕ (in degrees)
%   Output:
%     beta  - Turn-off angle β (in degrees), satisfying:
%             sin(α - ϕ) * exp(-(β - α)/tan(ϕ)) = sin(β - ϕ)

  % Convert angles from degrees to radians
  a = alpha * pi/180;
  p = phi   * pi/180;

  % Define the implicit equation f(beta) = 0
  f = @(b) sin(a - p).*exp( - (b - a)./tan(p) ) - sin(b - p);

  % Set initial guess b0: typically β > α, use α + π/2
```

```
b0 = a + pi/2;

  % Use fzero to solve (tolerant of small negative intervals)
  opts = optimset('Display','off');
  b_rad = fzero(f, b0, opts);

  % Convert radians back to degrees
  beta = b_rad * 180/pi;
end
```